ISSN:0971-1260
Vol-22-Issue-37-December -2019

Low temperature dc conductivity study of consolidated mercury selenide nanostructures

Subhojyoti Sinha

Department of Physics, School of Chemical Engineering and Physical Sciences, Lovely Professional University, Phagwara, Punjab, India.
corresponding author: sinha.23302@lpu.co.in

Abstract:

Mercury selenide nanostructures have been synthesized through a simple and convenient wet chemical route. The synthesized nanostructures have been characterized by X-ray diffraction (XRD), Uv-Vis spectroscopy and high resolution trnamission electron microscopy (HRTEM). The average partcile size is found to be 10.30 nm and the nanostrcures are polycrystalline in nature. The consolidated nanostrcures exhibits semiconducting behavior in the temperature range of $\mathbf{13}\boldsymbol{K} \leq \boldsymbol{T} \leq \mathbf{200}\boldsymbol{K}$. *The temperature variation of the conductivity has been analyzed in detail and it has been found that Mott's variable range hopping (VRH) conduction mechanism along with weak localization, charge carrier - charge carrier interaction have significant contributions, depending over the tempearture range.*

Keywords: Mercury selenide, dc conductivity, Variable range hopping conduction mechanism, Mott's charateristics temperature

1. Introduction

II-VI semiconducting nanoparticles have been of significant interest due to their wide existing and potential applications [1-4]. Among the different selenides cadmium selenide (CdSe), Zinc selenide (ZnSe) nanostructures have got tremendous attention due to their wide bandgap and size tunueable photoemission propeties [5-8]. This 'bandgap engineering' or control of particle size can be done meticulously by controlling the nucleation growth during synthesis procedure. The most common approach for the synthesis of nanostructured selenides is the 'organomettalic route'[9]. However as the route involves requirement of high temperature and highgly toxic materials like TOP/TOPOSe, some more greener route were later on invented and succesfully implemented yielding comparative results [10,11,12]. Again when the

ISSN:0971-1260
Vol-22-Issue-37-December -2019

nanocrystal's size becomes comparable to the excitonic bohr radius they are called quantum dots and due to the quantum confinement effect they shows off some scientifically interesting results. There are a lot of reports in the literature [13-16] about the nanostructures of silver selenide (Ag_2Se), Zinc selenide (ZnSe), lead selenide (PbSe), Nickel Selenide (NiSe) etc., but still the field of mercury chalcogenides are relatively unexplored. There are some reports on bulk mercury selenides (HgSe) whereas some reports focus mainly on the prepartion of HgSe nanostructures by different synthesis route like sonochemical method, hydrothermal method, wet chemical synthesis method, room temperature conversion route, using emulsion liquid membrane system or organomettalic route [17-20]. The toxicity of mercury may be one reason behind its limited study. However the behavior of this chalcogenide under quantum confinement is of particular interest and needs more attention. Here we report the synthesis of HgSe nanostructures in aqueous media at room temperature using thiyoglycolic acid (TGA) as the capping agent and dc conductivity variation in the temperature range $\mathbf{13}\boldsymbol{K} \leq \boldsymbol{T} \leq \mathbf{200}\boldsymbol{K}$. The consolidated nanostructures exhibits semiconducting behavior between 13 K to 200 K.

2. Experimental Methods

In a typical synthesis procedure, a stock solution of mercury precursor was prepared by dissolving 0.0125 mol of mercury chloride ($HgCl_2$) in 100 ml of de-ionized water, then adding equimolar amount of TGA under constant magnetic stirring. TGA reacts with $HgCl_2$ and forms a metal (Hg) complex. pH of the solution was then adjusted to 10.5 by adding 1M sodium hydorixed (NaOH) solution. This is marked as precursor A, a source of Hg^{++} ions. Sodium selenosulfate (Na_2SeSO_3) was used as a selnium precursor. For the preparation of Na_2SeSO_3 , 0.025 mol of Se powder and 6 gm sodium sulfite (Na_2SO_3) were mixed in 100 ml water and refulxed at 100^0 C for 2 hr [21]. The resultant, nearly transparent, solution was filtered and marked as the precursor B. In the next step precursor B was added slowly to precursor A under constant magnetic stirring at room temeprature. Allowing a reaction time of 15 min, the resultant black solution was centrifuged to obtain the black precipitate. It was then washed repeatedly with water, acetone and methanol and then dried under vacuum. The dried powder were then compacted into a pellet for electrical measurement.

ISSN:0971-1260
Vol-22-Issue-37-December -2019

3. Results and Discussion

The X-ray diffraction (XRD) patterns of the sample was studied with an PANalytical X'pert Pro MPD diffractometer with a step size of 0.05^0 (2θ) and step time 75 s from 15^0 to 90^0. The corresponding XRD pattern of the powder is shown in figure 1. It confirms the formation of cubic HgSe phase (ICSD code 24175) with space group F-43m.

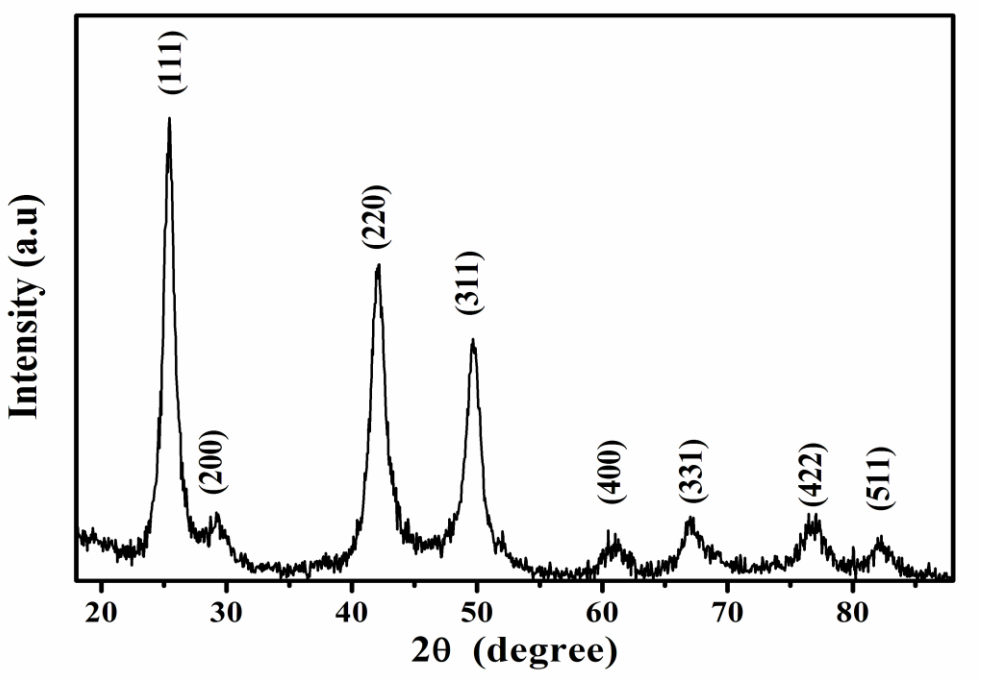

Figure 1: XRD pattern of the mercury selenide nanostructures

Transmission electron microscopic (TEM) image of the nanostructures is displayed in figure 2(a). Average particle size is calculated to be 10.3 nm. This is smaller than the excitonic Bohr radius of HgSe is 27 nm [17] which suggests that nanostructures are quantum dot in nature. The high resolution (HR)-TEM image of the sample along with the interplanar spacing shown in figure 2(b). In the inset of this image the selected area electron diffraction (SAED) pattern with marked diffracting planes is given. The SAED pattern suggests that the sample is polycrystalline in nature.

ISSN:0971-1260
Vol-22-Issue-37-December -2019

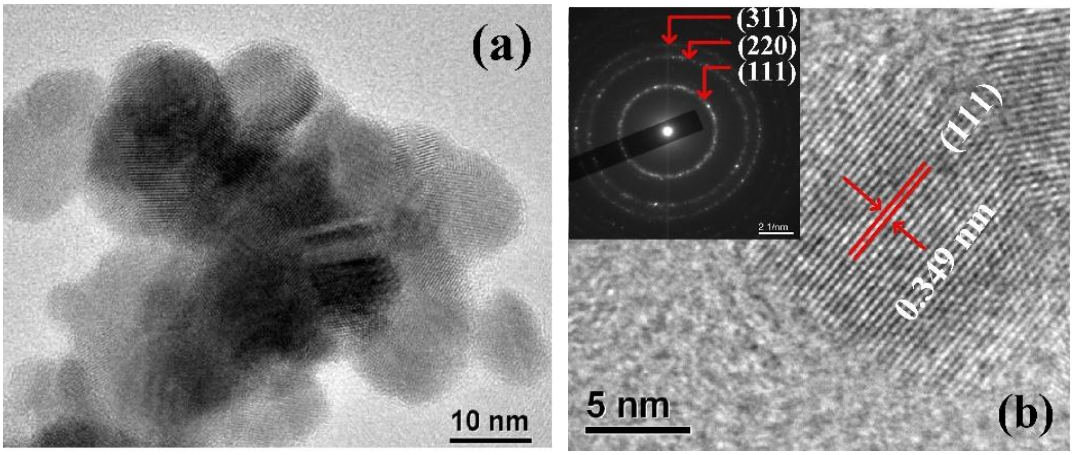

Figure 2: (a) TEM image of the HgSe nanostructures (b) HRTEM image showing the interplanar spacing and SAED pattern.

The ultraviolet-visible (Uv- vis) absorption spectra of the sample has been studied in the wavelength range of 300 nm–800 nm by dispersing the sample in ethanol and is shown in figure 3. The nanostructures exhibit a broad absorption peak at around 435 nm corresponding to band gap of 2.85 eV. Similar absorption edge and excitonic shoulder at around 3 eV was reported by Howes et al for TOPO capped HgSe quantum dots [17].

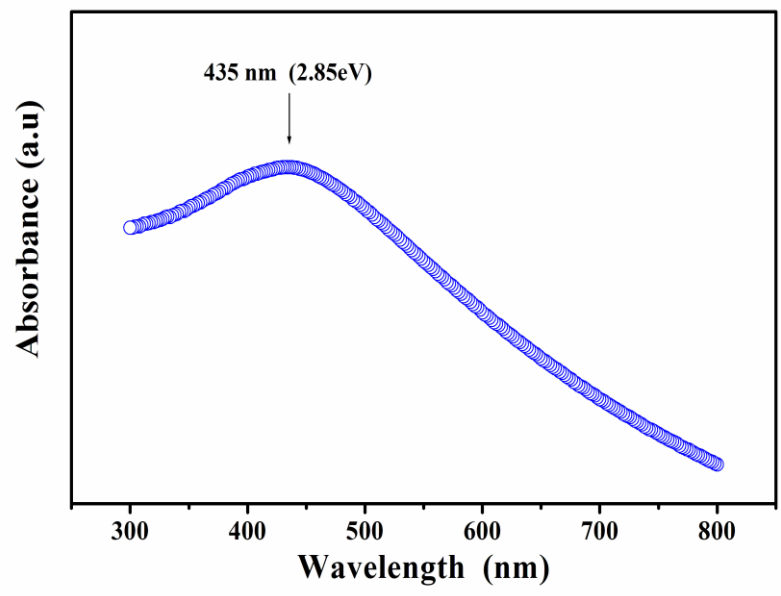

Figure 3: Uv-Vis absorption spectra of the HgSe nanostructures.

ISSN:0971-1260
Vol-22-Issue-37-December -2019

To study the dc conductivity (σ), the nanostructures were compressed to form a pellet with the help of a hydraulic press. The electrical measurement was carried out in a standard four probe method. The conductivity of the sample has been observed to increases with as the temperature increases from 13 K to 200 K exhibiting semiconducting behavior. This variation is plotted in figure 4. The temperature dependence of measured dc conductivity is found to be non-linear (inset of figure 4) indicating that Arrhenius law type behavior is not suitable to describe the observed temperature variation of conductivity. In Arrhenius law type conduction, there is thermal activation of charge carriers from valence band to the conduction band. The observed type of temperature dependence of conductivity can be can be explained considering the Mott's variable range hopping (VRH) model [22] which is expressed as- $\sigma_{dc}(T) = \sigma_0 \left(\frac{T_{Mott}}{T}\right)^{1/2} \exp\left[-\left(\frac{T_{Mott}}{T}\right)^{\gamma}\right]$ where σ_0 is a constant, Mott's characteristics temperature can be expressed as $T_{Mott} = \frac{16}{k_B N(\varepsilon_F) L^3_{loc}}$; k_B is Boltzmann

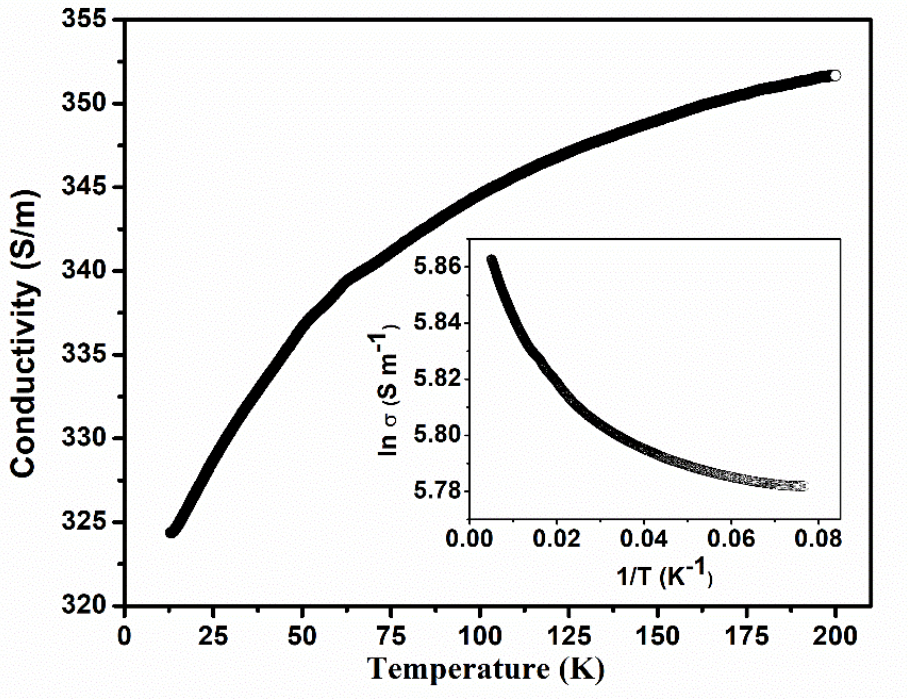

Figure 4: (a) Temperature variation of the dc conductivity of the consolidated HgSe nanostructures. Inset show the variation of lnσ with inverse of temperature.

ISSN:0971-1260
Vol-22-Issue-37-December -2019

constant, L_{loc} and $N(\varepsilon_F)$ denotes localization length and density of states at the Fermi level respectively and γ is the VRH exponent having values 1/4,1/3 and 1/2 for three (3D), two (2D) and one dimension (1D) respectively. It has been found that the plotting of ln $[T^{1/2}\sigma]$ versus $T^{-1/4}$ is comparatively more linear (figure 5) indicating that three-dimensional variable range hopping conduction mechanisms is possible in the studied case. However, the full measurement range cannot be fitted with this single mechanism. In fact, three-dimensional variable range hoping conduction mechanism play its role in the temperature range of 200 K to 57 K but fails for temperature lower than 57 K (as shown in figure 5).

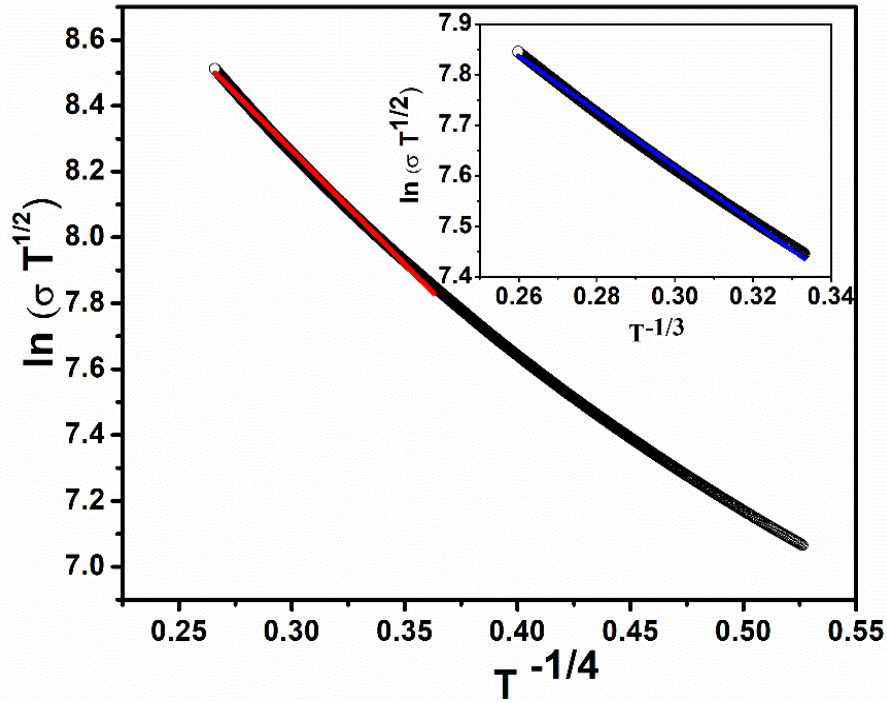

Figure 5: Plotting of temperature dependent dc conductivity as per Mott's VRH mechanism. The straight red line shows the theoretical fitting for 3D case. The inset shows the variation in the temperature range 27 K to 57 K as per the two-dimensional variable range hopping. The blue continuous line shows the theoretical fitting.

The Mott characteristics temperature in this temperature range (i.e. 200K to 57K) is found to be 2265 K. Interestingly in the range of 57K to 27K, two-dimensional

ISSN:0971-1260
Vol-22-Issue-37-December -2019

variable range (2D-VRH) hoping conduction mechanism has been found to play its role, having the value of Mott's characteristic temperature of 165 K. For the temperature below 27K it has been found that weak localization (WL) and charge carrier-charge carrier interaction becomes significant. At low temperatures, conductivity is decreased due to the occurrence of quantum interference phenomena [23], charge carrier-phonon and charge carrier-charge carrier couplings interaction. Coulomb interaction between the charge carriers also becomes significant.

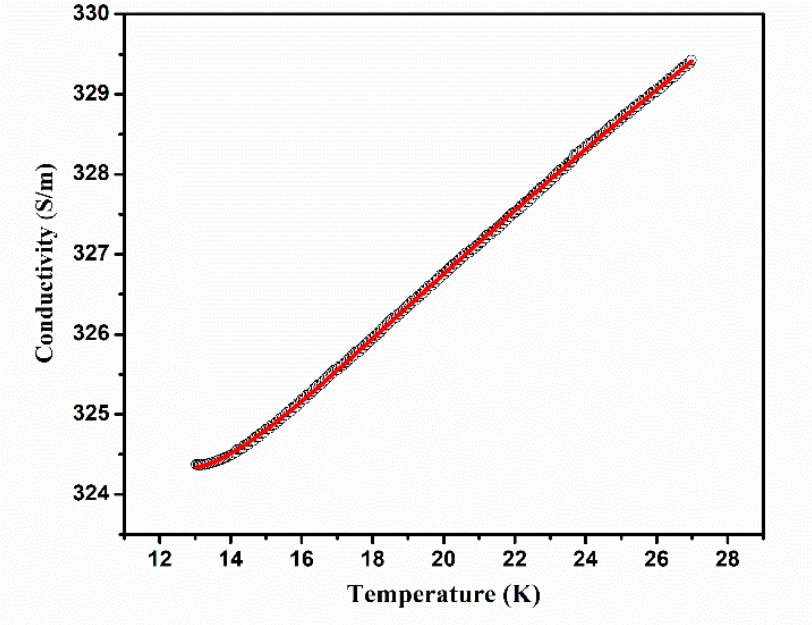

Figure 6: conductivity variation with temperature in the range 27 K to 13K. In this range weak localization and electron and electron interaction is prominent.

The combined effect of these effects can be expressed as [23,24] $\boldsymbol{\sigma(T) = \sigma(0) + aT^{\frac{1}{2}} + BT^{\frac{c}{2}}}$, where *a*, *B* and c are the parameters that depends on the extent of charge carrier-charge carrier interaction or phonon and extent of localization. This equation fits well in the low temperature conductivity data i.e in the temperature range of 27 K to 13 K and is shown in figure 6.

4. Conclusion

ISSN:0971-1260
Vol-22-Issue-37-December -2019

In this report, HgSe nanostructures have been successfully synthesized which exhibits a prominent absorption peak at around 435 nm. The compacted pellet of these nanostructures exhibits semiconducting behavior in the temperature $\mathbf{13K \leq T \leq 200K}$. From the analysis of the dc conductivity it has been observed that from 57 K to 200K Mott's three dimensional VRH mechanism is the prevailing charge transport mechanism whereas for 57K to 27 K it is Mott's 2-dimensional variable range conduction mechanism. This VRH mechanism fails to explain the observed variation in the temperature below 27 K which has been explained by the possible mechanism related to weak localization and charge carrier- charged carrier/phonon interaction. However, more work is needed to get the clear picture for the exact mechanism for the whole temperature range.

Acknowledgment: Author sincerely thanks Professor A.K. Meikap for his support during the work.

References:

[1] J. Lee, V. C Sundar, J. R. Heine, M. G. Bawendi, K. F. Jensen 'Full color emission from ii–vi semiconductor quantum dot–polymer composites', Adv. Mater., vol 12, pp.1102-1105, 2000,

[2] Jr. M. Bruchez, M. Moronne, P. Gin, S. Weiss, A. P. Alivisatos, ''Semiconductor nanocrystals as fluorescent biological labels'', Science, vol 281, pp. 2013-2016, 1998.

[3] X. Michalet, F. F. Pinaud, L. A. Bentolila, J. M. Tsay, S. Doose, J. J. Li, A. M. Wu, S. S. Gambhir and S. Weiss, "Quantum dots for live cells, in vivo imaging, and diagnostics", Science, vol. 307, pp. 538-544, 2005.

[4] J.G. Brennan, T. Siegrist, P. J. Carroll, S. M. Stuczynski, P. Reynders, L.E. Brus and M.L. Steigerwald, "Bulk and nanostructure Group II-VI compounds from molecular organometallic precursors" Chem. Mater. vol. 2, pp. 403-409, 1990.

[5] L. Zhao, L. Hu and X. Fang, "Growth and Device Application of CdSe Nanostructures" Adv. Funct. Mater. Vol 22, pp. 1551-1566, 2012.

[6] A.M. Smith, A.M. Mohs and S. Nie: 'Tuning the optical and electronic properties of colloidal nanocrystals by lattice strain', Nature Nanotechnol., vol. 4, pp. 56-63, 2009.

ISSN:0971-1260
Vol-22-Issue-37-December -2019

[7] I. Gur, N. A. Fromer, M. L. Geier and A. P. Alivisatos, "Air-stable all-inorganic nanocrystal solar cells processed from solution" Science vol. 310, pp. 462, 2005.

[8] G.-Y. Lan, Y.-W. Lin, Y.-F. Huang and H.-T. Chang, "Photo-assisted synthesis of highly fluorescent ZnSe(S) quantum dots in aqueous solution" J. Mater. Chem., vol. 17, pp. 2661–2666, 2007.

[9] C. B. Murray; D. J. Norris and M. G. Bawendi, "Synthesis and characterization of nearly monodisperse CdE (E= sulfur, selenium, tellurium) semiconductor nanocrystallites" J. Am. Chem. Soc., vol. 115, pp. 8706-8715, 1993

[10] A. L. Rogach, A. Kornowski, M. Gao, A. Eychmuller and H. Weller, ''Synthesis and characterization of a size series of extremely small thiol-stabilized CdSe nanocrystals'', *J. Phys. Chem. B, vol.* 103, pp. 3065-3069, 1999.

[11] W. Xu, Y. Wang, S. Liang, R. Xu, G. Zhang, F. Xu and D. Yin, ''Optimized synthesis and fluorescence spectrum analysis of CdSe Quantum Dots'' Journal of Dispersion Science and Technology, vol. 29, pp. 953-957, 2008.

[12] N.G. Semaltianos, S. Logothetidis, W. Perie, S. Romani, R. J. Potter, M. Sharp, P. French, G. Dearden, K. G. Watkins, ''CdSe nanoparticles synthesized by laser ablation'', Europhysics Letters, vol 84, pp. 47001, 2008.

[13] M.C. Santhosh Kumar and B. Pradeep, Materials Letters "Transport properties of silver selenide thin films from 100 to 300 K" vol. 56**,** pp. 491– 495, 2002.

[14] L. Yang, J. Zhu and D. Xiao, "Microemulsion-mediated hydrothermal synthesis of ZnSe and Fe-doped ZnSe quantum dots with different luminescence characteristics" RSC Adv., vol. 2, pp. 8179–8188, 2012.

[15] H.E. Romero and M. Drndic, "Coulomb Blockade and Hopping Conduction in PbSe Quantum Dots" Phys. Rev. Lett., vol. 95, pp. 156801, 2005.

[16] Z.-H. Han, S.-H. Yu, Y.-P. Li, H.-Q. Zhao, F.-Q. Li, Y. Xie, and Y.-T. Qian, "Convenient Solvothermal Synthesis and Phase Control of Nickel Selenides with Different Morphologies" Chem. Mater, vol. 11, pp. 2302-2304, 1999.

[17] P. Howes, M. Green, C. Johnston and A. Crossley, "Synthesis and shape control of mercury selenide (HgSe) quantum dots" J. Mater. Chem. Vol. 18 pp. 3474, 2008.

[18] N. Singh, K. R. Patil and P. K. Khanna, "Nano-sized HgSe powder: Single-step preparation and characterization" Materials Science and Engineering *B* vol 142 pp. 31, 2007.

ISSN:0971-1260
Vol-22-Issue-37-December -2019

[19] Y. Li, Y. Ding, H. Liao and Y. Qian, "Room-temperature conversion route to nanocrystalline mercury chalcogenides HgE (E=S,Se,Te)" , J. Phys. and Chemistry of Solids vol 60 pp. 965, 1999.

[20] S. B. Qadri, M. Kuno, C. R. Feng, B. B. Rath and M. Yousuf, "High temperature structural studies of HgS and HgSe quantum dots" Appl. Phys. Lett. Vol. 83, pp. 4011, 2003.

[21] S. Sinha, S. K. Chatterjee, J. Ghosh and A. K. Meikap, **"**Dielectric relaxation and ac conductivity behaviour of polyvinyl alcohol–HgSe quantum dot hybrid films" J. Phys. D: Appl. Phys. Vol. 47, pp. 275301, 2014.

[22] N. F. Mott and E. Davis, *Electronic process in nanocrystalline materials 2nd ed.* (Clarendron Press, Oxford,1979).

[23] V. P. Arya, V. Prasad and P. S. A. Kumar, Effect of magnetic field on Mott's variable-range hopping parameters in multiwall carbon nanotube mat, J. Phys.: Condens. Matter vol. 24 pp. 245602, 2012.

[24] P. Dai, Y. Zhang and M. P. Sarachik, **"**Electrical conductivity of metallic Si:B near the metal-insulator transition" Phys. Rev. B vol. 45 pp. 3984, 1992.